Journal of Materials Chemistry A

ROYAL SOCIETY OF CHEMISTRY

PAPER

Published on 28 July 2026

Cite this: DOI: 10.1039/d6ta04559f

AB-type monomer design for cleavable polyurethanes: conjugate substitution-induced main-chain scission for removable adhesives

Naoki Ohtani,[a] Yosuke Akae *[bcd] and Yasuhiro Kohsaka *[ae]

Polyurethanes that degrade *via* main-chain scission under ambient conditions were designed. Monomer precursors were synthesized *via* the Morita–Baylis–Hillman reaction of acrylates with terephthalaldehydic acid, followed by azidation. Subsequent Curtius rearrangement afforded AB-type monomers containing both isocyanate and hydroxy groups, and their self-polyaddition yielded a series of polyurethanes exhibiting solubility and glass transition temperatures depending on the structures of the pendant alkyl groups. Because the allylic positions of the methacrylate moieties were substituted with carbamate groups, treatment with diethylamine efficiently induced quantitative conjugate substitution under ambient conditions, resulting in main-chain scission accompanied by decarboxylation. Importantly, copolymers containing another AB-type monomer lacking methacrylate moieties underwent degradation *via* a self-immolative pathway triggered by conjugate substitution. The resulting polyurethanes functioned as adhesives for glass plates with a lap shear strength of 0.28 MPa and were readily removed by treatment with methanolic diethylamine solution.

Received 29th May 2026
Accepted 28th July 2026

DOI: 10.1039/d6ta04559f

rsc.li/materials-a

Yosuke Akae

Dr Yosuke Akae is currently a Junior Group Leader at RWTH Aachen University and a Specially Appointed Assistant Professor at the University of Osaka. After completing his PhD in 2016 under the supervision of Professor Toshikazu Takata at Tokyo Institute of Technology, he worked as an industrial researcher in Japan, a research associate at Tokyo Institute of Technology, a visiting researcher at Münster University with Professor Frank Glorius and at Shinshu University with Professor Yasuhiro Kohsaka, and later a JSPS Research Fellow (CPD) at Karlsruhe Institute of Technology with Professor Patrick Theato. His research focuses on the precise design and synthesis of sustainable and functional polymer materials, including supramolecular architectures.

Introduction

Cleavable polymers, which decompose into small molecules *via* specific stimuli, have gained attention from the perspective of sustainable society.[1,2] For example, polymers that recover the corresponding monomers or their precursors are promising for resource circulation *via* chemical recycling, and novel polymers with enhanced degradability,[3–8] including polymethacrylates,[9–12] polystyrenes,[13] polyesters,[14–16] and polycarbonates,[17] have been reported. On the other hand, cleavable polymers that undergo main-chain scission (MCS) to oligomers are also important, particularly as removable adhesives that allow component reuse and material recycling.[18–27] MCS efficiently releases polymer chains through a few bond-cleavage events from entanglement effects and intermolecular interactions.[28] As a result, drastic changes in polymer properties are caused, including the improvement of solubility,[29,30] decrease in solution viscosity,[31] and dissociation of self-assembly.[32] When MCS occurs in adhesives, such property changes decrease both cohesion and adhesion performances to achieve adhesion removal.[33] For example, Sato *et al.* reported linear polyperoxides synthesized from methyl sorbate and oxygen as detachable pressure-

[a]Faculty of Textile Science and Technology, Shinshu University, 3-15-1 Tokida, Ueda, Nagano 386-8567, Japan. E-mail: kohsaka@shinshu-u.ac.jp

[b]Department of Applied Chemistry, Graduate School of Engineering, The University of Osaka, 2-1 Yamadaoka, Suita, Osaka 565-0871, Japan

[c]Institute of Inorganic Chemistry, RWTH Aachen University, Landoltweg 1a, 52074 Aachen, Germany. E-mail: yosuke.akae@ac.rwth-aachen.de

[d]Institute for Chemical Technology and Polymer Chemistry (ITCP), Karlsruhe Institute of Technology (KIT), 76131 Karlsruhe, Germany

[e]Institute for Aqua Regeneration, Shinshu University, 3-15-1 Tokida, Ueda, Nagano 386-8567, Japan

sensitive adhesives (PSAs).[34] The polymer underwent MCS upon heating or UV irradiation, and the resulting oligomers behaved as plasticizers to reduce the cohesion force, leading to dismounting. In contrast, polymers that decompose into gaseous products are also effective for adhesion removal.[35,36]

Polyurethanes are among the most widely used polymers, ranking as the sixth most produced polymer worldwide, and are extensively utilized in applications such as foams, adhesives, and coatings.[20,37,38] However, the MCS of polyurethane *via* hydrolysis[39,40] and glycolysis[41,42] requires harsh conditions,[20] and other reactions for cleavage are desirable. In this context, Nozaki *et al.* reported the chemoselective cleavage of urethane linkages *via* hydrogenolysis using an iridium complex.[43] Another possible strategy for cleavable polyurethane is replacement of urethane bond with other weak analogues. For example, Li *et al.* introduced *tert*-butyl groups as *N*-substituents, enhancing the reversibility of urethane formation by huge steric hindrance.[44] Replacement of the carbonyl group in urethane bonds with a sulfonyl group is also a promising approach to enhance cleavability because 'sulfamate' bonds undergo hydrolysis more efficiently under mild conditions than carbamate, that is, urethane bonds.[45] These approaches achieve cleavability by directly altering the reactivity or chemical structure of the urethane-derived linkage.

In contrast to the above approaches, which target the urethane bond itself, we recently reported a strategy that places a conjugate-substitution trigger in the vicinity of the urethane bond (Fig. 1A).[46] In this reaction, a nucleophile attacks the electron-deficient *exo*-olefin of the methacrylate moiety rather than the urethane bond itself. The subsequent conjugate substitution induces cleavage of the allylic C–O bond, followed by decarboxylation and amine liberation. This reaction proceeds quantitatively under ambient conditions, even in aqueous media. Because this molecular design does not require direct modification or intrinsic weakening of the urethane bonds, the urethane groups remain intact before treatment with a nucleophile and continue to contribute to intermolecular interactions such as hydrogen bonding. For example, this strategy can be applied to polyurethane adhesives, in which hydrogen bonding between urethane groups plays a crucial role in determining the adhesion and cohesion strengths. That is, conjugate substitution triggers carbamate cleavage with CO_2 release, leading to debonding (Fig. 1B). Thus, this molecular design has the potential for application to removable polyurethane adhesives.

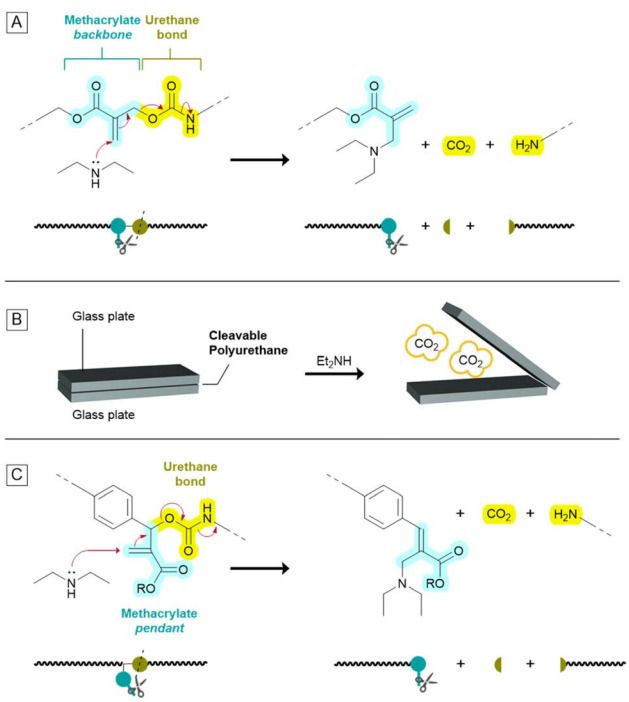

Fig. 1 (A) Design of cleavable polyurethane in our previous work. Both methacrylate moieties and urethane bonds are located in the backbone. (B) Debonding of removable polyurethane adhesives accompanied by CO_2 release. (C) Current molecular design that places methacrylate moieties as pendant groups.

However, several issues remain in implementing this strategy in polyurethane systems. In our previous molecular design, the methacrylate moieties, which function as triggers for the conjugate substitution reaction, were located in the backbone.[46] This structural limitation restricts the molecular design to tune polyurethane properties, particularly glass transition temperature (T_g) and affinity to substrates, which are important parameters for adhesives. In addition, the monomer was synthesized *via* Morita–Baylis–Hillman (MBH) reactions, which are intrinsically low in efficiency and result in low overall yields. To address these issues, we designed polyurethanes bearing methacrylate moieties as pendant groups (Fig. 1C). Although the monomers require MBH reactions for their preparation, the efficiency was significantly improved by using an electron-poor aldehyde. In addition, the present pendant-type design allows the ester alkyl substituent to be varied independently without altering the polyurethane backbone. Consequently, the thermal properties and solubility can be tuned while retaining MCS through conjugate substitution and the function of a removable adhesive. In this study, we report the polyurethane synthesis from AB-type monomers **5a–c** (Scheme 1) and their degradation *via* conjugate substitution reactions. The polymers undergo efficient cleavage under ambient conditions, enabling their application as removable adhesives, as demonstrated by debonding experiments.

Results and discussion

Monomer design and precursor synthesis

To realize the cleavable polyurethane design described in Fig. 1C, AB-type monomers **5a–c**, bearing isocyanate and hydroxy groups, were designed (Scheme 1). In this design, the methacrylate moiety responsible for conjugate substitution is located in the pendant group, while the ester alkyl substituent can be varied independently. Methyl, *n*-butyl, and *n*-dodecyl groups were selected as the alkyl pendants because the corresponding acrylates are commercially available and readily applicable to the present synthetic route. In addition, our previous study showed that the side-chain structure of related polyurethanes affects their T_g and solubility.[47,48] Thus, the

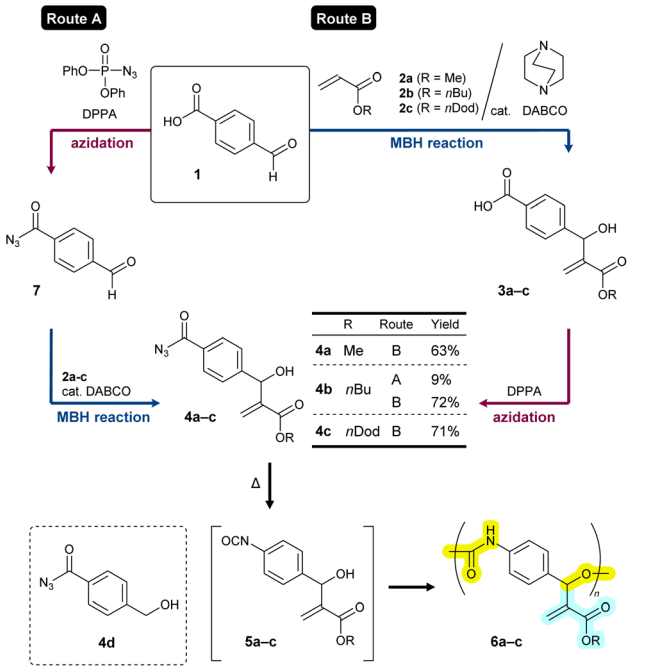

Scheme 1 Synthesis of cleavable polyurethane using AB-type monomers.

present homologous series was expected to enable a systematic evaluation of the influence of simple alkyl pendants on the properties of the resulting cleavable polyurethanes. Two synthetic routes were examined for **4b**, which is the precursor of **5b**. Route A involves the azidation of terephthalaldehydic acid (**1**) using diphenyl phosphoryl azide (DPPA) and the subsequent MBH reaction with *n*-butyl acrylate (**2b**). However, the overall yield was low (9%), and Route B, which consists of the opposite reaction sequence, was investigated. As described previously, typical MBH reactions suffer from low yields because of equilibrium and side reactions.[46] Nevertheless, MBH reactions using aromatic aldehydes substituted with electron-withdrawing groups proceed efficiently, as the reduced electron density at the carbonyl carbon facilitates nucleophilic attack.[49] In addition, the products were readily isolated without chromatographic purification or recrystallization, because impurities such as unreacted **1** and/or **2b** were removed by simple washing and precipitation processes. Thus, **3b** was isolated in high yield (78%), and azidation using DPPA afforded **4b** in 92% yield. That is, the overall yield of **4b** was 71%. Similarly, **4a** and **4c**, bearing methyl and *n*-dodecyl groups, respectively, were prepared in 63% and 71% yields, respectively. Similarly, **4d**, a monomer precursor without methacrylate moieties, was also prepared. The structures of the obtained products were characterized by ^{1}H and ^{13}C NMR and FTIR spectroscopies (Fig. S1–S24).

Homopolymerization

According to previous reports,[47,48,50,51] monomer precursors **4a–c** were heated at 110 °C for 30 min to induce the Curtius rearrangement, generating **5a–c**, followed by polymerization (Scheme 1 and Table 1). We initially examined the

Table 1 One-pot preparation and polymerization of **5a–c** and control monomer **5d**

Entry[a]	4	Solv.[b]	Catalyst[c]	Yield (%)	M_n[d] (g mol^{-1})	$Đ$[d]
1	**4b**	—	—	88	4000	1.5
2	**4b**	—	DBTDL	93	11 000	1.8
3	**4b**	DMF	—	79	3600	1.6
4	**4b**	DMF	DBTDL	96	4600	1.6
5	**4a**	—	DBTDL	98	Insoluble	
6[e]	**4a**	—	DBTDL	90	4700	1.6
7[e]	**4b**	—	DBTDL	90	9200	1.8
8[e]	**4c**	—	DBTDL	94	11 000	1.8
9	**4d**	DMF	—	84	25 000	3.0

[a] Curtius rearrangement followed by self-polyaddition were conducted in bulk or in DMF at 110 °C for 30 min. [b] DMF (1.0 mL for 1.0 mmol of **4**) was used in Entries 3, 4 and 9. [c] [**4**]/[DBTDL] = 50/1. [d] Determined by SEC (DMF, 40 °C, polystyrene standards). [e] Reactions were conducted at 90 °C for 180 min.

polymerization behavior of **4b**. Bulk polymerization at 110 °C resulted in a number-average molar mass (M_n) and dispersity in molar mass ($Đ$) of 4000 g mol^{-1} and 1.5, respectively (Entry 1). The chemical structure of the product was characterized as **6b** using ^{1}H NMR spectroscopy (Fig. 3C, see 'main-chain scission' subsection). Polymerization using di-*n*-butyl tin dilaurate (DBTDL) resulted in a higher M_n (Entry 2), whereas those in *N*,*N*-dimethylformamide (DMF) did not achieve a higher M_n (Entries 3 and 4). Thus, polymerization using **4a** was conducted under a condition similar to that used for Entry 2; however, the product was insoluble in DMF, dimethyl sulfoxide (DMSO), tetrahydrofuran (THF), and chloroform ($CHCl_3$), which prevented its characterization (Entry 5). As described later, the expected product, **6a**, underwent thermal decomposition at temperatures above 150 °C. This suggests that the polymerization product might have undergone thermal decomposition owing to the reaction heat during bulk polymerization. To avoid such concerns, the polymerization of **4a–c** was performed at 90 °C for 180 min on a ten-gram scale, resulting in the expected polyurethanes (Entries 6–8). Notably, the M_n values of polyurethanes **6a–c** were lower than that of polyurethane **6d**, which was derived from precursor **4d** without any substituent (Scheme 1, Entry 9). Thus, the lower M_n values were attributed to the secondary alcohol moieties of **5a–c**, which are generally less reactive than primary alcohols owing to steric hindrance.[47,48,52] The polymer structures were characterized using ^{1}H and ^{13}C NMR spectroscopies (Fig. S25–S32) and size-exclusion chromatography (SEC; Fig. S34–S37).

Solubility, thermal, and viscoelastic properties

The introduction of a pendant group significantly affected the polymer solubility and thermal properties (Table 2). **6a** and **6b** were soluble in DMSO, DMF, acetone, and THF, but insoluble in diethyl ether (Et_2O) and chloroform (Table S1). In contrast, **6c** was soluble in acetone, Et_2O, THF, partly soluble in DMF, and insoluble in DMSO and chloroform. These differences indicate the effects of alkyl pendants on the solubility of polyurethanes.

Table 2 Solubility and thermal properties of obtained homopolymers

	Solubility[a]					
code	DMSO	DMF	Acetone	Et_2O	T_g[b] (°C)	T_{d5}[c] (°C)
6a	+	+	+	—	(92)[d]	146
6b	+	+	+	—	93	146
6c	—	+/−	+	+	51	161
6d	+/−	+/−	—	—	—	174

[a] Solubility was evaluated using 5 mg of polymer in 1.0 mL. +: Soluble, +/−: partly soluble, −: insoluble. [b] Determined from the midpoint of the heat capacity change in the second DSC heating scan (10 °C min^{-1}, N_2 atmosphere). [c] Determined by TGA (10 °C min^{-1}, N_2 atmosphere). [d] Onset temperature of glass transition.

6d did not exhibit a glass transition below the decomposition temperature, whereas the DSC profiles of **6a–c** indicated a glass transition (Fig. 2A). Because the glass transition of **6a** occurred at temperatures near the thermal decomposition temperature, only the onset of the glass transition could be reliably determined at 92 °C. The T_g values of **6a–c** decreased with increasing alkyl pendant length (Table 2). These results imply that the pendant groups effectively weaken interchain interactions, such as hydrogen bonding between urethane groups.

The thermal decomposition behavior was not significantly affected by pendant groups. **6a–c** exhibited significant weight loss over 130–170 °C in the thermogravimetric analysis (TGA) profiles (Fig. 2B and S39–S41). A similar drastic weight loss was also observed for **6d**, a self-immolative polymer (SIP) that undergoes depolymerization triggered by external stimuli (Fig. 2C).[53,54] Thus, the thermal decomposition was anticipated to originate from depolymerization, which is accompanied by CO_2 elimination. Indeed, the weight loss of **6a** was 18%, which agreed with the weight fraction of the CO_2 moiety in the urethane bonds.

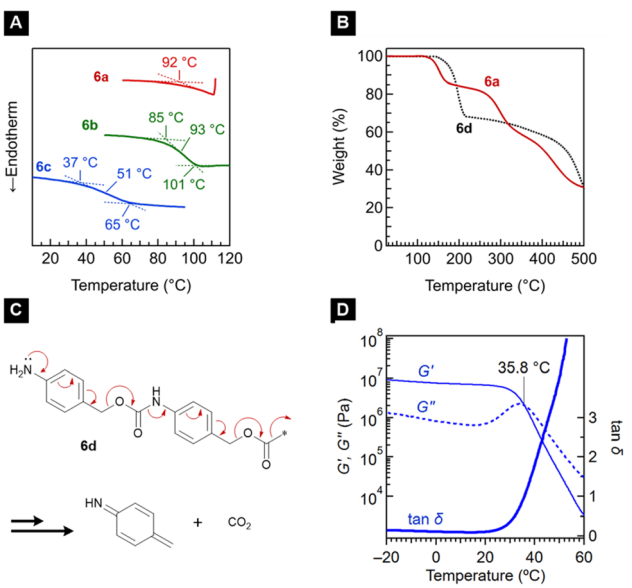

Fig. 2 (A) DSC profiles of **6a–c**. (B) TGA profiles of **6a** and **6d**. (C) Reaction mechanism of self-immolation of **6d**. (D) Temperature-sweep rheology curves of **6c** during cooling.

To evaluate the rheological properties, film preparation was attempted by casting solutions of **6a–c** in acetone (300 mg mL^{-1}), although **6a** and **6b** were too brittle and did not afford self-supporting films. In contrast, **6c** afforded a self-supporting film with a thickness of approximately 0.35 mm (Fig. S45). This difference suggests that the long alkyl pendant of **6c** improved the film-forming behavior. The temperature-sweep rheology curve of **6c** (Fig. 2D) indicated that the storage modulus (G') at 20 °C was 6.6 MPa, suggesting a glassy property. However, G' and the loss modulus (G'') crossed at approximately 36 °C, which was corresponding to glass transition observed in the DSC curve. Above this temperature, the loss modulus exceeded the storage modulus, indicating that viscous behavior became dominant. Because the T_g of **6c** was close to ambient temperature, **6b** was used for the adhesion tests discussed later.

Main-chain scission *via* conjugate substitution

Because **6a–c** contain methacrylate moieties bearing allylic carbamate leaving groups, nucleophilic conjugate substitution at the *exo*-olefin moiety can directly induce cleavage of the polyurethane main chain, as shown in Fig. 1C. Specifically, nucleophilic addition to the electron-deficient *exo*-olefin is followed by allylic C–O bond cleavage and decarboxylation of the resulting carbamic acid intermediate. To investigate this reaction, **6b** was treated with diethylamine (Et_2NH) in DMSO-d_6 at 25 °C (Fig. 3A). Size-exclusion chromatography (SEC) profiles indicated a rapid decrease in the molar mass within 30 min (Fig. 3B). The ^1H NMR spectra changed completely after 24 h (Fig. 3C). For example, the vinylidene proton signals A (5.8 ppm) and B (6.3 ppm) disappeared after 24 h, whereas a new signal at 3.2 ppm, assignable to the allylic protons, appeared. The conversion of the methacrylate moieties in **6b**, estimated as the intensity decrease of signal A relative to that of DMF as an internal standard, exceeded 50% within 5 min and reached nearly 100% within 6 h (Fig. 3D). The second-order kinetic plot (Fig. 3E) showed a linear relationship until the conversion reached 98%, suggesting that degradation proceeds *via* MCS through a conjugate substitution reaction. Similar experiments were conducted using propylamine (nPrNH$_2$), triethylamine (Et_3N), and 1,4-diazabicyclo[2.2.2]octane (DABCO) to investigate the effects of amine structure on the degradation rate. As described previously, MCS using Et_2NH was almost complete within 6 h (Fig. S46). In contrast, propylamine required approximately 24 h (Fig. S55–S58). Moreover, the conversion was only 70% even after 24 h when Et_3N was used as the nucleophile (Fig. S59–S62). This tendency can be explained by the differences in nucleophilicity determined from the electron density and steric hindrance. Notably, quantitative conversion was achieved within 4 h when DABCO, the most nucleophilic amine examined, was used (Fig. S63–S66). The ^1H NMR spectrum after 24 h (Fig. S65), assigned with reference to the literature,[55] indicated two major products, **8b** and **11b**. Thus, the reaction pathway was suggested as shown in Scheme 2. That is, the conjugate substitution with DABCO resulted in an ammonium

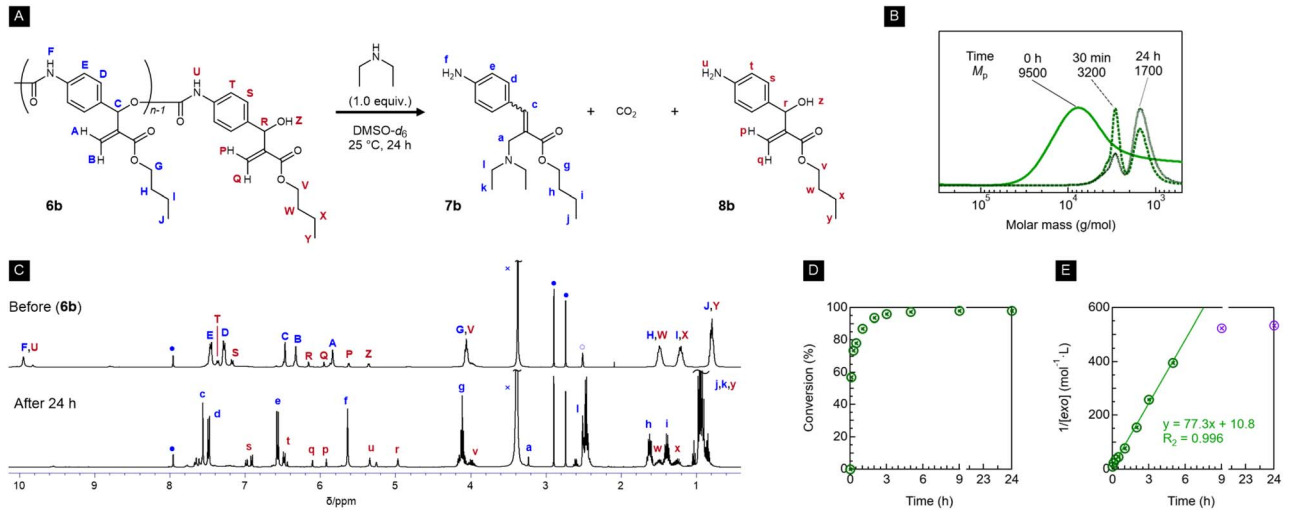

Fig. 3 MCS reaction of **6b** using Et_2NH. (A) Reaction scheme. (B) SEC profile changes. (C) ^1H NMR spectral changes. (D) Time *versus* conversion plot. (E) Second order kinetics plot.

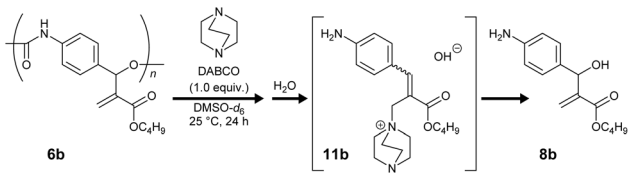

Scheme 2 Proposed reaction pathway in MCS of **6b** using DABCO as a nucleophile.

intermediate **11b**, and further conjugate substitution with water or hydroxide ion resulted in **8b**. The MCS using Et_2NH as a nucleophile was also effective for **6a** and **6c** in DMSO-d_6 and acetone-d_6, respectively (Fig. S47–S54).

Copolymer synthesis, properties, and main-chain scission

To understand the effects of methacrylate moieties on polymer synthesis, properties, and degradation, the copolymerization of **5b** and **5d** was conducted by heating the corresponding precursors **4b** and **4d** in DMF at 110 °C for 30 min (Scheme 3). Copolymerization was performed with varied feed ratios, and copolymers with the expected compositions were obtained (Table 3, Entries 10–12; Fig. S33 and S38). The T_g values of the obtained copolymers increased from 38 to 67 °C as the composition of **5d** units increased from 50 to 90 mol% (Fig. S44). The MCS reactions of the obtained copolymers **6b**/**d** were investigated in a manner similar to that used for the homopolymers. For example, the copolymer obtained in Entry 10 (**5b**-units: 50 mol%) was treated with Et_2NH at 25 °C. The SEC profile changes clearly indicated the progress of the MCS reaction after 24 h (Fig. S72), whereas the ^1H NMR spectrum suggested the complete disappearance of the vinylidene proton signals (Fig. S67). These results suggest that the MCS was completed after 24 h. To quantitatively evaluate the degradability of copolymers, the ratio of M_n after 24 h to that at 0 h was used as an index (Fig. 4A). This ratio decreased with increasing **5b**-units, suggesting that the incorporation of **5b** units effectively introduces cleavage points into the polymer backbone.

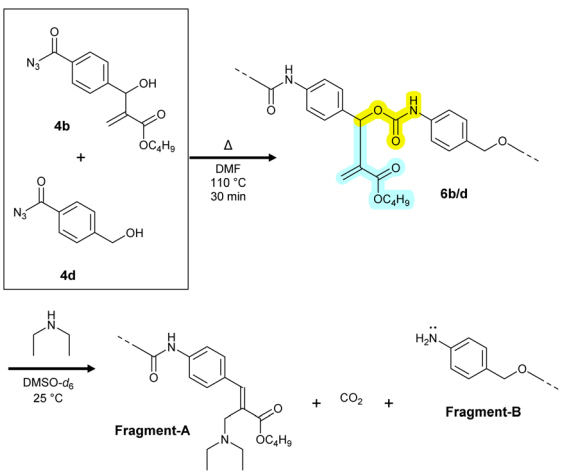

Scheme 3 Synthesis and MCS of **6b**/**d**.

Table 3 One-pot preparation and copolymerization of **5b** and **5d**

	Feed (mol%)						
Entry[a]	**5b**	**5d**	Yield (%)	M_n[c] (g mol^{-1})	$Đ$[b] (–)	T_g[c] (°C)	T_{d5}[d] (°C)
10	50	50	89	4400	1.7	38	137
11	30	70	90	6700	1.9	42	135
12	10	90	91	8200	2.2	67	146
13[e]	9	91	99	12 000	2.1	69	170

[a] Curtius rearrangement of **4b** and **4d** followed by polyaddition of their products **5b** and **5d** were conducted in DMF at 110 °C for 30 min. [b] Determined by SEC (DMF, 40 °C, polystyrene standards). [c] Determined by DSC (second heating, 10 °C min^{-1}, N_2 atmosphere). [d] Determined by TGA (10 °C min^{-1}, N_2 atmosphere). [e] Polymerization was conducted in DMF at 100 °C for 60 min.

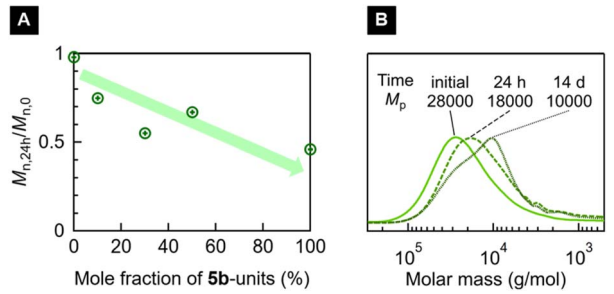

Fig. 4 (A) Effects of copolymer composition on M_n after MCS for 24 h. (B) SEC profile changes during MCS of **6b**/**d** (**5b**-unit: 9 mol%) using Et_2NH (1.0 equiv.).

It is notable that **6b**/**d** (**5b**-unit: 9 mol%), obtained *via* polymerization at 100 °C for 60 min (Entry 13), underwent quantitative MCS after 24 h. Nevertheless, a further decrease in the molar mass was observed after 14 d (Fig. 4B). Thus, another reaction mechanism is required to explain this slow decrease in molar mass. A possible scenario is the spontaneous depolymerization of Fragment-B, derived from the MCS reaction, as a SIP (Fig. 2C). This phenomenon is interesting but out of the main topic of this study, removable adhesives, and will be reported in our future work.

Application to removable adhesives

To demonstrate the potential application as a removable adhesive, the bonding and subsequent debonding of two glass substrates were examined. An acetone solution of **6b** (300 mg mL^{-1}) was applied to one glass substrate to obtain an adhesion area of 625 mm^2, and another glass substrate was placed on top of it. The lap shear strength was 0.28 MPa (Fig. 5A). The adhesive joint was immersed in a 50 wt% solution of Et_2NH in methanol at 25 °C. One of the glass substrates detached under its own weight after 1 h (Video-1), and no visible adhesive residue remained on the glass surface after debonding (Fig. 5B). Gas bubble formation was observed from the adhesive layer during immersion (Video-1). In contrast, a similar experiment using pure methanol also resulted in debonding, but it took a longer time (5–6 h), and a large amount of adhesive residue was observed (Fig. 5C). These results suggest that the MCS reaction effectively reduced the cohesion of the adhesive layer, possibly through decreased chain entanglements and disruption of hydrogen bonding between urethane groups, thereby enabling rapid and clean debonding.

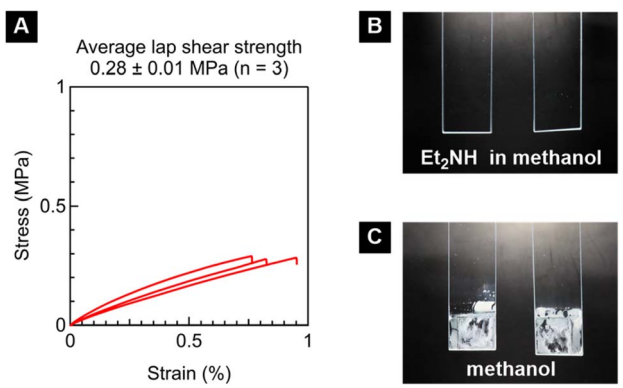

Fig. 5 Lap-shear stress–strain curves of glass/glass joints (A). Adhesive residue after immersion in a Et_2NH/methanol solution (B) and methanol (C).

To evaluate the adhesion of **6b** to different substrate materials, glass/steel, glass/PMMA, and glass/wood joints were prepared. The glass/steel joint exhibited lap shear strength of 0.43 MPa (Fig. S76), whereas the glass/PMMA and glass/wood joints detached upon the application of a small force and could not be subjected to lap shear testing. These results indicate that the adhesion performance of **6b** depends on the substrate material. The debonding behavior of the glass/steel joint was also evaluated. The joint debonded after 30 min in a 50 wt% solution of Et_2NH in methanol at 25 °C (Video-2, Fig. S77A), whereas a longer time (6–7 h) was required in pure methanol and a large amount of adhesive residue remained (Fig. S77B). These results indicate that the MCS reaction is also effective for the rapid and clean debonding of glass/steel joints.

Conclusions

A series of polyurethanes bearing methacrylate moieties in pendant groups were prepared from AB-type monomer precursors **4a–c** *via* Curtius rearrangement and polyaddition. The obtained polymers **6a–c** exhibited solubilities and T_g values reflecting the pendant chain lengths, whereas the tune of T_g values was achieved *via* copolymerization with non-substituted monomer **5d**. Thus, the present pendant-type design allows polyurethane properties to be tuned by changing the ester alkyl substituent without altering the polyurethane backbone. These polymers readily decomposed *via* the MCS reaction based on conjugate substitution with primary, secondary, and tertiary amines, even at ambient temperature. In addition, copolymer **6b**/**d**, which contains non-substituted units derived from **5d**, showed a further decrease in molar mass after the initial MCS, probably because of the self-immolation mechanism. The polymer was applied as a removable adhesive for glass plates because the MCS reaction proceeded under ambient conditions. Treatment with a methanolic diethylamine solution enabled rapid and clean debonding without visible adhesive residue. These results suggest that MCS reduced the cohesive strength of the adhesive layer through decreased chain entanglements and disruption of hydrogen bonding. Because debonding proceeds under ambient conditions without heating, the present approach may be useful for bonded assemblies containing heat-sensitive or dissimilar components. We believe that this concept will contribute to the establishment of a sustainable society.

Author contributions

NO: data curation, formal analysis, investigation, validation, funding acquisition, visualization, methodology, writing – draft. YK: conceptualization, funding acquisition, project

administration, resources, supervision, writing – – review & editing. YA: conceptualization, methodology, supervision, writing – review and editing.

Conflicts of interest

NO, YA, and YK have filed a patent in Japan on polyurethanes reported here (JP Patent Application No. 2026-27706).

Data availability

The data supporting this manuscript is available as part of the supplementary information (SI). Supplementary information: experimental procedure, ^{1}H and ^{13}C NMR spectra, FTIR spectra, SEC profiles, TGA profiles, and DSC profiles. See DOI: https://doi.org/10.1039/d6ta04559f.

Acknowledgements

This work was financially supported by JST SPRING, Japan Grant Number JPMJSP2144 (Shinshu University; for NO) and by a project (JPNP18016) commissioned by the New Energy and Industrial Technology Development Organization (NEDO; for YK) and by International Polyurethane Technology Foundation (for YK). YA appreciates support of the Werner Siemens Foundation in the frame of the WSS Research Centre "catalaix".

Notes and references

1 C. Lefay and Y. Guillaneuf, *Prog. Polym. Sci.*, 2023, **147**, 101764.
2 S. Bag, D. Ghosh, S. Banerjee and P. De, *ACS Appl. Polym. Mater.*, 2025, **7**, 14033–14061.
3 A. J. Christy and S. T. Phillips, *Sci. Adv.*, 2023, **9**, eadg2295.
4 Y. Chiba, S. Hirabayashi and Y. Kohsaka, *Polym. Chem.*, 2026, **17**(16), 1562–1568.
5 Y. Chiba, R. Kawatani and Y. Kohsaka, *ACS Macro Lett.*, 2023, **12**, 1672–1676.
6 X. Y. Oh, Y. Ge and A. Goto, *Chem. Sci.*, 2021, **12**, 13546–13556.
7 A. Kazama and Y. Kohsaka, *Polym. Chem.*, 2019, **10**, 2764–2768.
8 M. Hong and E. Y. X. Chen, *Green Chem.*, 2017, **19**(16), 3692–3706.
9 R. W. Hughes, T. Maity, T. Sergent, A. H. Balzer, I. S. Zastrow, M. S. Patel, L. M. Baker, P. M. Keown, L. T. J. Korley and B. S. Sumerlin, *J. Am. Chem. Soc.*, 2025, **147**, 19485–19490.
10 R. W. Hughes, M. E. Lott, I. S. Zastrow, J. B. Young, T. Maity and B. S. Sumerlin, *J. Am. Chem. Soc.*, 2024, **146**, 6217–6224.
11 M. T. Chin, T. Yang, K. P. Quirion, C. Lian, P. Liu, J. He and T. Diao, *J. Am. Chem. Soc.*, 2024, **146**, 5786–5792.
12 Y. Chiba, S. Hirabayashi and Y. Kohsaka, *Chem. Sci.*, 2025, **16**, 12804–12811.
13 J. B. Young, J. I. Bowman, M. E. Lott, L. A. Diodati, K. C. Stevens, R. W. Hughes, L. E. Mann, A. H. Balzer, L. T. J. Korley and B. S. Sumerlin, *ACS Macro Lett.*, 2025, **14**, 576–581.
14 X. Zhang, W. Guo, C. Zhang and X. Zhang, *Nat. Commun.*, 2023, **14**, 5423.
15 Q. Yan, J. Ma, W. Pei, Y. Zhang, R. Zhong, S. Liu, Y. Shen and Z. Li, *Angew. Chem., Int. Ed.*, 2025, **64**, e202418488.
16 X. Y. Tang, M. Hong, L. Falivene, L. Caporaso, L. Cavallo and E. Y. X. Chen, *J. Am. Chem. Soc.*, 2016, **138**, 14326–14337.
17 T. Abe, R. Takashima, T. Kamiya, C. P. Foong, K. Numata, D. Aoki and H. Otsuka, *Green Chem.*, 2021, **23**, 9030–9037.
18 K. R. Mulcahy, A. F. R. Kilpatrick, G. D. J. Harper, A. Walton and A. P. Abbott, *Green Chem.*, 2022, **24**, 36–61.
19 C. T. de M. Soares, M. Ek, E. Östmark, M. Gällstedt and S. Karlsson, *Resour., Conserv. Recycl.*, 2022, **176**, 105905.
20 G. Rossignolo, G. Malucelli and A. Lorenzetti, *Green Chem.*, 2024, **26**, 1132–1152.
21 G. Oliveux, L. O. Dandy and G. A. Leeke, *Prog. Mater. Sci.*, 2015, **72**, 61–99.
22 E. Bezeraj, S. Debrie, F. J. Arraez, P. Reyes, P. H. M. Van Steenberge, D. R. D'hooge and M. Edeleva, *RSC Sustainability*, 2025, **3**, 1996–2047.
23 D. L. Thompson, J. M. Hartley, S. M. Lambert, M. Shiref, G. D. J. Harper, E. Kendrick, P. Anderson, K. S. Ryder, L. Gaines and A. P. Abbott, *Green Chem.*, 2020, **22**, 7585–7603.
24 C. S. Gonzalez, A. Basdeo, F. A. Cruz Sanchez, C. Nouvel, J. M. Pearce and H. Boudaoud, *Sustainable Mater. Technol.*, 2025, **44**, e01430.
25 X. Wen, S. S. Bae and M. L. Rivera, in *Proceedings of the 2025 CHI Conference on Human Factors in Computing Systems*, ACM, New York, NY, USA, 2025, pp. 1–21.
26 A. M. Mineo and R. Katsumata, *Angew. Chem., Int. Ed.*, 2024, **63**, e202316248.
27 G. R. Kiel, D. J. Lundberg, E. Prince, K. E. L. Husted, A. M. Johnson, V. Lensch, S. Li, P. Shieh and J. A. Johnson, *J. Am. Chem. Soc.*, 2022, **144**, 12979–12988.
28 D. Messmer, O. Bertran, R. Kissner, C. Alemán and A. D. Schlüter, *Chem. Sci.*, 2019, **10**, 6125–6139.
29 A. Rathore, I. Pollentier, H. Singh, R. Fallica, D. De Simone and S. De Gendt, *J. Mater. Chem. C*, 2020, **8**, 5958–5966.
30 Y. Kohsaka, K. Toyama, M. Kawauchi and K. Naganuma, *ACS Macro Lett.*, 2024, 1016–1021.
31 A. Tayal and S. A. Khan, *Macromolecules*, 2000, **33**, 9488–9493.
32 Y. Men, T. G. Brevé, H. Liu, A. G. Denkova and R. Eelkema, *Polym. Chem.*, 2021, **12**, 3612–3618.
33 Y. Kohsaka and K. Naganuma, *ACS Polym. Au*, 2025, **5**, 481–487.
34 E. Sato, H. Tamura and A. Matsumoto, *ACS Appl. Mater. Interfaces*, 2010, **2**, 2594–2601.
35 T. Sasaki, S. Hashimoto, N. Nogami, Y. Sugiyama, M. Mori, Y. Naka and K. V. Le, *ACS Appl. Mater. Interfaces*, 2016, **8**, 5580–5585.
36 M. Iseki, Y. Hiraoka, C. Jing, H. Okamura, E. Sato and A. Matsumoto, *J. Appl. Polym. Sci.*, 2018, **135**, 46252.
37 J. O. Akindoyo, M. D. H. Beg, S. Ghazali, M. R. Islam, N. Jeyaratnam and A. R. Yuvaraj, *RSC Adv.*, 2016, **6**, 114453–114482.

38 A. Das and P. Mahanwar, *Adv. Ind. Eng. Polym. Res.*, 2020, **3**, 93–101.
39 J. L. Gerlock, J. Braslaw, L. R. Mahoney and F. C. Ferris, *J. Polym. Sci., Polym. Chem. Ed.*, 1980, **18**, 541–557.
40 Z. Dai, B. Hatano, J.-I. Kadokawa and H. Tagaya, *Polym. Degrad. Stab.*, 2002, **76**, 179–184.
41 H. Beneš, R. Černá, A. Ďuračková and P. Látalová, *J. Polym. Environ.*, 2012, **20**, 175–185.
42 P. Jutrzenka Trzebiatowska, H. Beneš and J. Datta, *React. Funct. Polym.*, 2019, **139**, 25–33.
43 T. Iwasaki, Y. Yamada, N. Naito and K. Nozaki, *J. Am. Chem. Soc.*, 2024, **146**, 25562–25568.
44 F. Wang, W. Gao and C. Li, *Chin. Chem. Lett.*, 2024, **35**, 109305.
45 S. Das, K. Doktor, B. Saha, F. C. Sousa E Silva, R. M. Wynn and Q. Michaudel, *Angew. Chem., Int. Ed.*, 2025, **64**, e202510841.
46 T. Noda, A. Tanaka, Y. Akae and Y. Kohsaka, *RSC Adv.*, 2023, **13**, 20336–20341.
47 Y. Shen, P. Theato and Y. Akae, *Macromolecules*, 2024, **57**, 8162–8175.
48 X. Kneidl, L. Forkel, T. Cui, P. Theato and Y. Akae, *J. Polym. Sci.*, 2026, **64**, 366–375.
49 S. Kunnikuruvan, S. Batra and N. N. Nair, *ChemPhysChem*, 2012, **13**, 3723–3730.
50 Y. Akae and P. Theato, *J. Polym. Sci.*, 2024, **62**, 4127–4135.
51 J. Reeb, Y. Shen, P. Theato and Y. Akae, *Macromolecules*, 2025, **58**, 2701–2708.
52 X. Kneidl, J. Reeb-Begic, T. Cui, P. Theato and Y. Akae, *Polym. Chem.*, 2026, **17**(23), 2423–2436.
53 O. Shelef, S. Gnaim and D. Shabat, *J. Am. Chem. Soc.*, 2021, **143**, 21177–21188.
54 R. E. Yardley, A. R. Kenaree and E. R. Gillies, *Macromolecules*, 2019, **52**, 6342.
55 P. S. Addy, M. Shivrayan, M. Cencer, J. Zhuang, J. S. Moore and S. Thayumanavan, *ACS Macro Lett.*, 2020, **9**, 855–859.

